

Chapter 9 Conclusions

9.1 Summary of results

The MINOS experiment has been designed with a baseline of 731 km and a mean neutrino interaction energy of 17 GeV. These parameters have been chosen to explore the region of neutrino oscillation parameter space suggested by the atmospheric neutrino anomaly.

The neutrino mixing parameters are not well measured by the atmospheric neutrino experiments if the anomaly is interpreted in terms of neutrino oscillations. The size of the discrepancy between the experiments and the Monte Carlo predictions indicates that the mixing matrix elements are large although flux uncertainties, large statistical errors and measurement errors on the direction of the incoming neutrino mean that it is difficult to distinguish between $\nu_\mu \rightarrow \nu_e$ and $\nu_\mu \rightarrow \nu_\tau$ oscillations. In addition, the value of Δm^2 is not well measured (it is uncertain to ± 1 decade or more). This uncertainty in Δm^2 means that the average MINOS L/E might not be optimal to measure the mixing parameters responsible for the atmospheric neutrino anomaly. It is therefore essential that there is flexibility in the MINOS beam design, and that the capability exists to switch to a lower energy beam if required.

This thesis has shown how well the mixing parameters could be measured by MINOS if the atmospheric neutrino anomaly is due to neutrino oscillations. The most important (and convincing) measurement that MINOS could make is the observation of an

energy-dependent suppression of the ν_μ flux. For large mixing, this would be an unambiguous demonstration of neutrino oscillations. It has been shown in Chapter 4 that MINOS could provide a precision measurement of Δm^2 ($< 10\%$ error) if the true value lies between $0.005 < \Delta m^2 < 0.2 \text{ eV}^2$ for the default WBB. The performance of a proposed low energy beam, which is designed to confront the new Super-Kamiokande atmospheric neutrino results, has been studied in Chapter 5. This beam allows a measurement of Δm^2 down to approximately 0.002 eV^2 . Further results are needed before the optimal beam design for MINOS becomes clear. The results from atmospheric neutrino experiments are subject to large systematic uncertainties and they may not provide decisive information before 2002. The long-baseline K2K experiment, however, is expected to run in 1998-1999 and could see a statistically significant L/E dependent effect if $\Delta m^2 \sim 0.01 \text{ eV}^2$.

The low energy beam has a much reduced flux compared to the default three horn WBB, which would limit the potential reach in parameter space. In addition, switching from the default beam design to the low energy beam would require a major redesign of the beam line and has serious implications for the COSMOS experiment (the number of neutrinos above tau production threshold and hence the sensitivity of COSMOS to $\nu_\mu \rightarrow \nu_\tau$ oscillations would be greatly reduced). It may be too late to implement the low energy beam for 2002 but it should remain an option as a possible upgrade path. For the three horn beam, work on reducing both the rate uncertainties to $< 4\%$ and the uncertainties in the prediction of the far detector spectrum for no oscillations to less than 20% of their current value would reduce parameter measurement errors and minimise the risk of observing spurious neutrino oscillation signals if the atmospheric neutrino anomaly is not explained by neutrino mixing.

The second important measurement that MINOS could make is of the matrix elements that relate the flavour and mass eigenstates. It has been shown in Chapter 6 that it is

possible to identify electron neutrino events in MINOS so a three-generation analysis of MINOS data is possible. The nature of the analysis depends on the results of other experiments and the value of Δm^2 measured by MINOS, as will be explained in the following section. A general three-flavour analysis involving six free parameters most easily explains the current data (although even this may be insufficient if the LSND result is confirmed) but an analysis of MINOS (or any other experiment) in this space is difficult. The analysis described in Chapter 7 assumes the simplifying one mass-scale dominance model. This model, which assumes a neutrino mass hierarchy that is similar to the charged leptons and quarks, is suggested by the results of the atmospheric and solar neutrino experiments. The analysis has indicated how well the parameters could be measured and has shown that, for any three-flavour mixing hypothesis, MINOS (or any other experiment with a single flavour beam) will at best isolate two solutions for the mixing matrix elements. This uncertainty is a fundamental property of three-generation mixing in the OMSD model. Since the CHOOZ result has effectively ruled out the prospect of observing large $\nu_\mu \rightarrow \nu_e$ mixing in MINOS, the role of MINOS (in addition to checking the CHOOZ result) is to measure or constrain the amount of $\nu_\mu \rightarrow \nu_e$ mixing. It has been shown in Chapter 7 that it is possible in principle to distinguish between two-generation $\nu_\mu \rightarrow \nu_\tau$ and three-generation mixing and still be consistent with the CHOOZ limit.

General three-flavour mixing allows for the possibility of leptonic CP violation. Chapter 7 has studied the prospects of observing a CP violating effect in MINOS. For favourable values of the parameters (threefold maximal mixing and both Δm^2 's $\sim 10^{-2}$ eV²) it has been shown that the energy distributions of electron-like events for ν_μ and $\bar{\nu}_\mu$ runs are a more convincing demonstration of CP violation than the difference in oscillation probabilities. The prospects for observing CP violation, however, depend critically on the values of Δm^2 and the mixing matrix elements. MINOS could only observe CP violation if

both Δm^2 's $> 10^{-3} \text{ eV}^2$ and all the matrix elements are large. The prospects for this are not favourable due to the value of Δm^2 obtained by fits to solar neutrino results and the CHOOZ limit, which appear to rule out the prospects of observing any significant CP violation in MINOS for any three-flavour mixing scenario.

If the evidence from CHOOZ is combined with that from the atmospheric neutrino experiments then it appears that large $\nu_\mu \rightarrow \nu_\tau$ mixing is likely. If this is the case then it is important for MINOS to have the ability to detect tau leptons. Since MINOS is relatively coarsely grained, it is impossible to do this on an event by event basis. Chapter 8 describes a statistical method to observe tau leptons by relying on differences in event topologies between tau? hadrons and NC events (the major source of background). While this test has low efficiency ($\tau \rightarrow \pi\nu$ efficiency $\sim 2\%$) and a signal to background ratio of one, it benefits somewhat from finer transverse and longitudinal granularity. Since the ratio of ν_τ / ν_μ charged-current cross sections depends on neutrino energy, the $\tau \rightarrow \pi$ analysis is strongly dependent on the value of Δm^2 . If $\Delta m^2 \sim 10^{-3} \text{ eV}^2$ (as suggested by the preliminary Super-Kamiokande atmospheric neutrino results) then the $\tau \rightarrow \pi$ test will not observe a signal because almost all of the ν_τ are below tau production threshold. On the other hand, if $\Delta m^2 \geq 10^{-2} \text{ eV}^2$ then a five standard deviation or greater effect may be observed.

Figure 9.1 summarises many of the results presented in this thesis. The figure shows how the expected size of measurement errors and ν_τ appearance signals depend on the value of Δm^2 if oscillations are assumed with large $\sin^2 2\theta$. The top two lines in Figure 9.1 show the range of Δm^2 for which a precision measurement ($< 10\%$ error) of the mixing parameters is possible in the low energy beam, as described in Chapter 5. The lines assume neutrino oscillations with $\sin^2 2\theta = 0.7$ and a 20 kiloton year exposure of MINOS. The third and fourth lines show the range of Δm^2 for which a precision measurement is possible in the

three horn wide band beam for the ν_μ CC energy analysis that is described in Chapter 4. These lines assume neutrino oscillations with $\sin^2 2\theta = 0.7$ and a 3.3 kiloton year exposure of MINOS. The fifth and sixth lines are the analogue of the fourth and fifth lines for the ν_e appearance analysis that is described in Chapter 5. The bottom line shows the range of Δm^2 for which a five standard deviation or greater effect in the $\tau \rightarrow \pi$ analysis is expected, assuming an exposure of 20 kiloton years. All the lines assume that the number of events expected for no oscillations is perfectly known.

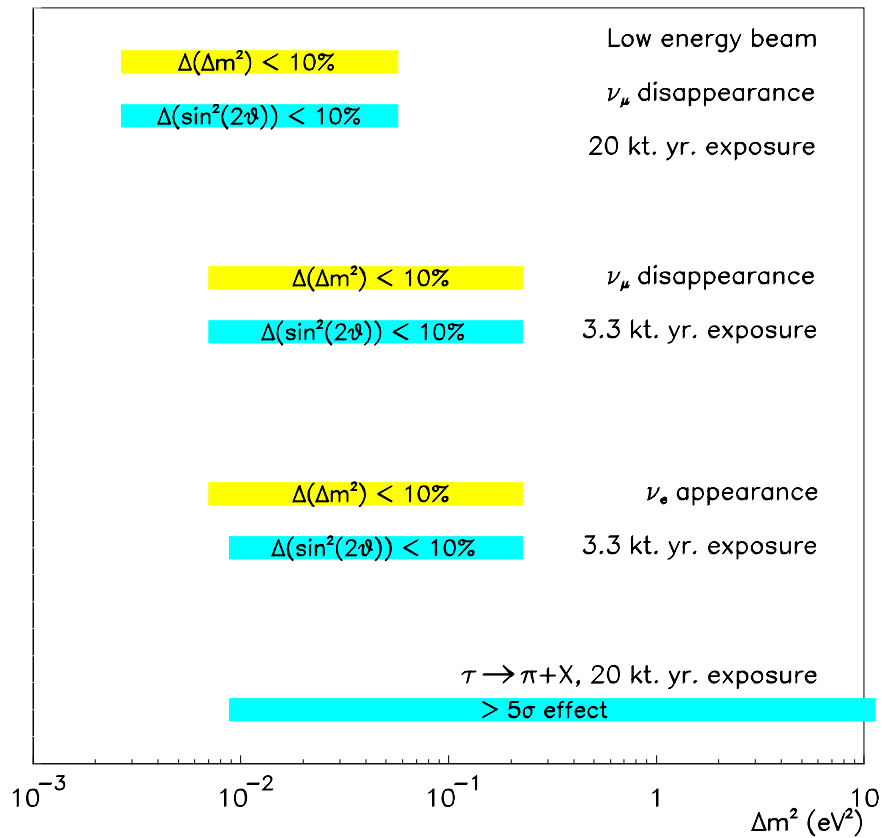


Figure 9.1 – A summary of the major results of this thesis. The lines are explained in the accompanying text.

The figure shows that, if the results of the three horn wide band beam and the possible low energy beam are combined, the MINOS experiment could measure the mixing parameters with $< 10\%$ errors if neutrino oscillations occur with $\sin^2 2\theta \geq 0.7$ and $0.003 \leq \Delta m^2 \leq 0.1 \text{ eV}^2$. This range covers much of the region of parameter space suggested by the atmospheric neutrino anomaly although the low energy beam is vital for a measurement of the lowest values of Δm^2 suggested by the anomaly ($\Delta m^2 \sim 0.003 \text{ eV}^2$). The $\tau \rightarrow \pi$ analysis can provide complementary information on the oscillation mode if $\Delta m^2 > 0.01 \text{ eV}^2$.

It is clear that an all-encompassing fit that combines the energy information from the ν_μ and ν_e CC energy tests (and possibly the rate and energy information from the $\tau \rightarrow \pi$ test) in a three-generation framework will use the flavour and energy information from MINOS in the most efficient way and produce the smallest errors on the mixing parameters. The strategy of dividing the analysis into a number of discrete but complementary parts (Chapter 4-8 of this thesis) is useful in a) testing the no-oscillation hypothesis, b) measuring (or setting limits on) the mixing parameters and the oscillation mode and c) understanding and correcting for any sources of systematic error which may be different for the various analyses. The all-encompassing analysis can be performed in the future when the results of the simpler analyses are understood.

9.2 MINOS and neutrino oscillation phenomenology

This section briefly reviews the current experimental hints of neutrino oscillations and explains how they are related to the future results of MINOS. Four possible mixing scenarios are presented that can explain most, if not all, of these hints and the consequences of these scenarios for MINOS are discussed.

9.2.1 Recap of experimental hints for neutrino oscillations

The LSND excess

LSND observes an excess of events that are consistent with $\bar{\nu}_e$ CC interactions, as described in section 2.5.4. This can be explained by $\bar{\nu}_\mu \rightarrow \bar{\nu}_e$ oscillations with $P(\bar{\nu}_\mu \rightarrow \bar{\nu}_e) \sim 0.3\%$ [49]. Much of the allowed region in neutrino oscillation parameter space has been excluded by other experiments although a small region survives at $\Delta m^2 \sim 1 \text{ eV}^2$ and $\sin^2 2\theta \sim 10^{-2}$.

The atmospheric neutrino anomaly

The anomalous flavour ratio of atmospheric neutrinos can be interpreted in terms of $\nu_\mu \rightarrow \nu_\tau$ or $\nu_\mu \rightarrow \nu_e$ oscillations with $\sin^2 2\theta \sim 1$ and $\Delta m^2 > 10^{-3} \text{ eV}^2$, as described in section 2.5.2. The $\nu_\mu \rightarrow \nu_e$ solution has recently been ruled out by the CHOOZ experiment which has set a limit of $\sin^2 2\theta < 0.18$ at 90% C.L. for $\nu_\mu \rightarrow \nu_e$ oscillations with $\Delta m^2 > 10^{-3} \text{ eV}^2$ [47].

The Kamiokande and Super-Kamiokande atmospheric neutrino experiments both observe that the flavour ratio of atmospheric neutrinos depends on the zenith angle, and hence L/E . The best-fit values of Δm^2 are $\Delta m^2 \sim 10^{-2} \text{ eV}^2$ for the Kamiokande data [41] and $\Delta m^2 \sim 2 - 3 \times 10^{-3} \text{ eV}^2$ for the Super-Kamiokande data [36]. The combined results of these two experiments suggest that Δm^2 lies in the range $10^{-3} < \Delta m^2 < 10^{-1} \text{ eV}^2$.

The solar neutrino problem

Five experiments observe a flux of solar neutrinos that is significantly lower than the prediction of the standard solar model (the suppression is between a factor of two and a

factor of four). The suppression of the neutrino flux also appears to depend on neutrino energy (as shown in Table 2.1).

These observations can be explained by $\nu_e \rightarrow \nu_x$ oscillations with large mixing strength. There are three possible regions of Δm^2 :

1. $\Delta m^2 \sim 10^{-3} \text{ eV}^2$: this assumes vacuum oscillations with $\sin^2 2\theta \sim 1$. The suppression of neutrino flux is energy independent, and hence somewhat inconsistent with the results of Table 2.1, because:

$$\frac{\Delta m^2 L}{E} \sim \frac{10^{-3} \times 10^{11}}{1} \gg 1.$$

2. $\Delta m^2 \sim 10^{-5} \text{ eV}^2$: this assumes MSW resonant neutrino oscillations, as described in section 2.5.1.2. Two solutions are possible; the small angle solution with a vacuum mixing angle of $\sin^2 2\theta \sim 10^{-2}$, and the large angle solution with $\sin^2 2\theta \sim 1$. The suppression of neutrino flux can be energy dependent and the current data is therefore well-described by these models.
3. $\Delta m^2 \sim 10^{-10} \text{ eV}^2$: this assumes vacuum oscillations with $\sin^2 2\theta \sim 1$. The value of Δm^2 is tuned to the Sun-Earth distance ($\Delta m^2 L / E \sim 1$) so the suppression of neutrino flux is energy dependent. This solution predicts a seasonal variation in the neutrino flux over and above that expected from the eccentricity of the Earth's orbit, as described in section 2.5.1.2.

9.2.2 Implications of current results for MINOS

LSND and MINOS

The LSND excess suggests $\bar{\nu}_\mu \rightarrow \bar{\nu}_e$ oscillations with $\Delta m^2 \sim 1 \text{ eV}^2$ and $\sin^2 2\theta \sim 10^{-2}$. MINOS is expected to be sensitive to $\nu_\mu \rightarrow \nu_e$ oscillations with $\sin^2 2\theta > 3 \times 10^{-3}$ [72] and so the size of any possible $\nu_\mu \rightarrow \nu_e$ signal in MINOS from the LSND result is small.

If the value of Δm^2 from the LSND analysis is also responsible for the atmospheric neutrino anomaly (i.e. the anomaly is explained by $\nu_\mu \rightarrow \nu_\tau$ oscillations with $\Delta m^2 \sim 1 \text{ eV}^2$ and $\sin^2 2\theta \sim 1$) then MINOS would observe a large suppression in the ν_μ CC event rate but would not be able to measure Δm^2 because the oscillation phase would be smeared out by experimental energy resolution (see section 4.5.3). This scenario would require the Kamiokande and Super-Kamiokande zenith angle distributions of atmospheric neutrinos to be wrong.

The atmospheric neutrino anomaly and MINOS

This has been discussed in detail in the preceding chapters of this thesis. If the atmospheric neutrino anomaly is due to neutrino oscillations and the CHOOZ result is taken into account then $\nu_\mu \rightarrow \nu_\tau$ oscillations with $\sin^2 2\theta \sim 1$ and $\Delta m^2 > 10^{-3} \text{ eV}^2$ are implied. In this case MINOS should see a large suppression of the ν_μ CC event rate and measure the mixing parameters to better than 10% accuracy, as demonstrated in Chapter 4.

The solar neutrino problem and MINOS

The solar neutrino data is well-described by neutrino oscillations with $\Delta m^2 \sim 10^{-5} (10^{-10}) \text{ eV}^2$. These values of Δm^2 have implications for MINOS; they imply that, even if the atmospheric neutrino anomaly is explained by neutrino mixing with $\Delta m^2 \sim 10^{-2} \text{ eV}^2$, the expected CP violating amplitude in MINOS cannot be larger (and is expected to be much smaller) than $10^{-5} (10^{-11}) / 10^{-2} < 10^{-3}$ and is hence unobservable.

9.2.3 Implications for MINOS of possible neutrino oscillation scenarios

Several example neutrino oscillation scenarios that can explain most, if not all, of the hints that are summarised in section 9.2.1 are listed in Table 9.1. The values of the independent Δm^2 's for each scenario are listed in the top row of the table. The table shows whether the scenarios can explain the three experimental hints of neutrino oscillations listed in the first column; the LSND excess, the atmospheric neutrino anomaly and the solar neutrino problem. It is also shown whether or not the scenarios are consistent with the zenith angle distribution of atmospheric neutrinos from Kamiokande and Super-Kamiokande. This is indicated by a tick or a cross in the fourth row of the table. The oscillation modes for each of the hints are shown in the table if they can be explained by the scenarios and a cross is shown if they cannot. The prospect of observing a CP violating in MINOS for each of the scenarios is shown in the sixth row of the table; a cross indicates that the predicted CP violating amplitude is unobservable in MINOS ($D_{\mu e} < 10^{-3}$). The seventh row suggests the appropriate analysis for MINOS; 'OMSD' means that the three-flavour one mass-scale dominance model can be adopted, '6 parameter' means that a generalised three-flavour framework with three mixing angles, a complex phase and two independent values of Δm^2 is necessary, and '> 3 flavour' means that a complex analysis involving the three standard generations plus a sterile neutrino is required.

	Scenario 1 $\Delta m^2_{32} \sim 0.01$ $\Delta m^2_{21} \sim 10^{-5}$ or (10^{-10})	Scenario 2 $\Delta m^2_{32} \sim 1$ $\Delta m^2_{21} \sim 10^{-5}$	Scenario 3 $\Delta m^2_{32} \sim 10^{-3}$ $\Delta m^2_{21} \sim 10^{-3}$	Scenario 4 $\Delta m^2_{43} \sim 1$ $\Delta m^2_{32} \sim 0.01$ $\Delta m^2_{21} \sim 10^{-5}$ or 10^{-10}
LSND	×	$\bar{\nu}_\mu \rightarrow \bar{\nu}_e$	×	$\bar{\nu}_\mu \rightarrow \bar{\nu}_e$
Atmospheric neutrino anomaly	$\nu_\mu \rightarrow \nu_\tau$	$\nu_\mu \rightarrow \nu_\tau$	$\nu_\mu \rightarrow \nu_\tau$ 3 flavour	$\nu_\mu \rightarrow \nu_\tau$ or $\nu_\mu \rightarrow \nu_{sterile}$
Kamiokande and Super-K zenith angle distributions	✓	×	✓	✓
Solar neutrinos	$\nu_e \rightarrow \nu_\mu$ MSW or vacuum oscillations	$\nu_e \rightarrow \nu_\tau$ small angle MSW oscillations	Vacuum oscillations, three-flavour mixing	$\nu_e \rightarrow \nu_{\tau,sterile}$ MSW or vacuum oscillations
CP violation in MINOS	×	×	×	Possible [90]
MINOS analysis	OMSD	OMSD	6 parameter	> 3 flavour

Table 9.1 – Four possible neutrino oscillation scenarios.

Figure 9.2 shows how the values of Δm^2 chosen in the four scenarios correspond to the experimental data. The abscissa of the plot is L/E , which corresponds to $(\Delta m^2)^{-1}$. The labels below the axis show the regions of L/E that are relevant to the experimental hints for neutrino oscillations. There are two regions for solar neutrinos, corresponding to the MSW and vacuum oscillation solutions respectively. The thick line between $10 < L/E < 10^3$ km/GeV shows the region of Δm^2 , and hence L/E , suggested by the Kamiokande and Super-Kamiokande zenith angle distributions of atmospheric neutrinos. The values of Δm^2 or L/E that explain the various experimental hints for the four scenarios are shown by the markers. If a marker for a particular hint is absent then the hint cannot be explained by the particular scenario (for example, scenario 1 cannot explain the LSND excess and hence the open circle, which represents LSND, is absent). In some scenarios (one and four), the solar neutrino problem can be solved by either of two values of Δm^2 . The

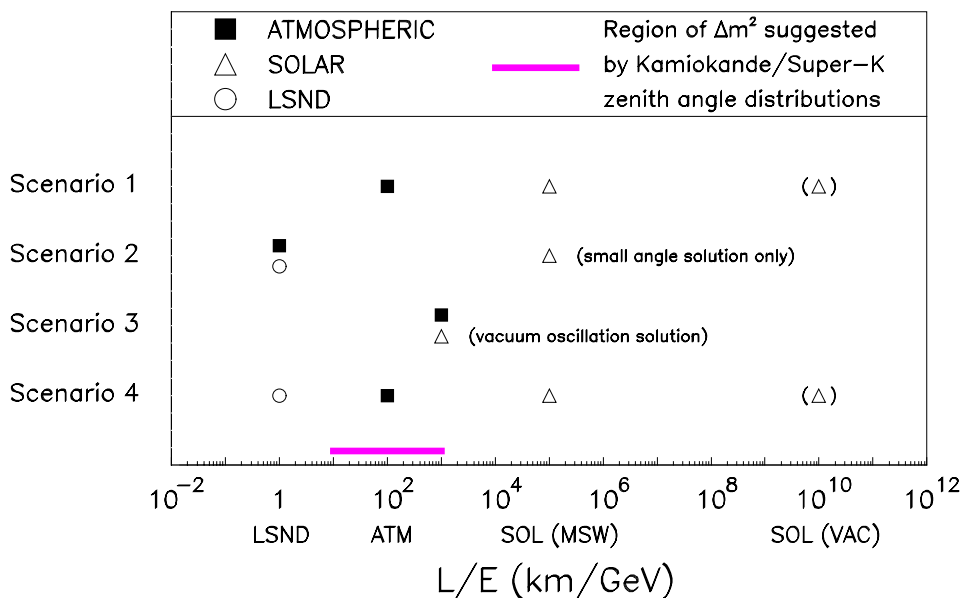


Figure 9.2 – The values of L/E (or $(\Delta m^2)^{-1}$) required to solve the experimental hints of neutrino oscillations, for the scenarios listed in Table 9.1.

second value of Δm^2 is indicated in parentheses for these cases. In scenario 2, the atmospheric neutrino anomaly is explained by oscillations with large Δm^2 ($\sim 1 \text{ eV}^2$) and the fact that the black square, which represents the atmospheric neutrino anomaly, is inconsistent with the range of L/E suggested by the zenith angle distributions of Kamiokande and Super-Kamiokande (the thick line) means that these distributions are assumed to be spurious in this model.

The first scenario can be regarded as the most plausible three-generation solution, given the current weight of evidence and assuming that the LSND excess is spurious. The second and third scenarios are other three-generation solutions that require at least one piece of evidence for neutrino oscillations to be wrong. The fourth scenario assumes that three independent mass-scales are required to explain all the data. This requires at least four neutrino generations. All of the scenarios assume that the atmospheric neutrino anomaly is genuine and therefore a large neutrino oscillation effect is expected to be observed in MINOS. If the neutrino masses are strongly ordered ($m_3 \gg m_2 \gg m_1$), as suggested by the charged lepton and quark sectors, then scenarios 2 and 4 imply neutrino masses that are cosmologically interesting ($m_\nu \sim 1 \text{ eV}^2$). If the masses are degenerate, then all the scenarios may imply that neutrinos possess a significant fraction of the mass density of the universe.

The detailed predictions and consequences of the four scenarios are described in the following sections.

Scenario 1: LSND spurious, hierarchical mass spectrum

$$\Delta m_{32}^2 \sim 10^{-2} \text{ eV}^2, \Delta m_{21}^2 \sim 10^{-5} (10^{-10}) \text{ eV}^2$$

LSND: the LSND excess is assumed to be spurious.

ATMOSPHERIC: the atmospheric neutrino anomaly is explained by $\nu_\mu \rightarrow \nu_\tau$ oscillations with $\Delta m^2 \sim 10^{-2} \text{ eV}^2$ and $\sin^2 2\theta \sim 1$.

SOLAR: the solar neutrino problem is solved by either MSW enhanced neutrino oscillations with $\Delta m^2 \sim 10^{-5} \text{ eV}^2$ (large or small angle solution) or vacuum oscillations with $\Delta m^2 \sim 10^{-10} \text{ eV}^2$ and $\sin^2 2\theta \sim 1$. The suppression of solar neutrino flux can (in principle) be energy dependent.

MINOS ANALYSIS STRATEGY: the values of the two independent Δm^2 's allows the one mass-scale dominance (OMSD) model to be applied. MINOS is expected to observe large $\nu_\mu \rightarrow \nu_\tau$ mixing and small or zero $\nu_\mu \rightarrow \nu_e$ mixing, due to the CHOOZ result.

CP VIOLATION: the values of Δm^2 assumed here rule out the possibility of observing a CP violating amplitude in MINOS.

Scenario 2: Large Δm^2 atmospheric neutrino oscillations, hierarchical mass spectrum

$$\Delta m_{32}^2 \sim 1 \text{ eV}^2, \Delta m_{21}^2 \sim 10^{-5} \text{ eV}^2$$

LSND: the LSND excess is explained by $\bar{\nu}_\mu \rightarrow \bar{\nu}_e$ oscillations with $\Delta m^2 \sim 1 \text{ eV}^2$ and $\sin^2 2\theta \sim 10^{-2}$.

ATMOSPHERIC: the atmospheric neutrino anomaly is explained by $\nu_\mu \rightarrow \nu_\tau$ oscillations with $\Delta m^2 \sim 1 \text{ eV}^2$ and $\sin^2 2\theta \sim 1$. This value of Δm^2 is not consistent with the zenith angle distributions of atmospheric neutrinos observed by the Kamiokande and Super-Kamiokande experiments and they are thus assumed to be spurious.

SOLAR: the solar neutrino problem is solved by $\nu_e \rightarrow \nu_\tau$ oscillations with $\Delta m^2 \sim 10^{-5}$ and $\sin^2 2\theta \sim 10^{-2}$ (the small angle MSW solution). The suppression can be energy dependent.

MINOS ANALYSIS STRATEGY: the OMSD model can be applied in this case. The value of Δm^2 is too large to be measured directly by MINOS but large effects will be seen in many of the MINOS oscillation tests. The $\tau \rightarrow \pi + X$ test is also expected to yield a six standard deviation effect here.

CP VIOLATION: the value of Δm^2 required to solve the solar neutrino problem rules out the possibility of observing CP violation in MINOS.

Scenario 3: LSND spurious, non-hierarchical mass spectrum

$$\Delta m_{32}^2 \sim 10^{-3} \text{ eV}^2, \Delta m_{21}^2 \sim 10^{-3} \text{ eV}^2$$

LSND: the LSND excess is assumed to be spurious.

ATMOSPHERIC: the atmospheric neutrino anomaly is explained by neutrino oscillations with $\Delta m^2 \sim 10^{-3} \text{ eV}^2$ and large mixing. The oscillation mode ($\nu_\mu \rightarrow \nu_e$, $\nu_\mu \rightarrow \nu_\tau$ or three-flavour mixing) is not constrained because the value of Δm^2 is below the limit set by the CHOOZ experiment. The value of Δm^2 is consistent with the Super-Kamiokande zenith angle distribution and marginally consistent with that for Kamiokande.

SOLAR: the solar neutrino problem is solved by vacuum oscillations with $\Delta m^2 \sim 10^{-3} \text{ eV}^2$ and large mixing (the oscillation mode is not constrained). This solution predicts that the oscillation probability is energy independent and so is somewhat inconsistent with the current solar neutrino data (as shown by Table 2.1).

MINOS ANALYSIS STRATEGY: since the two values of Δm^2 are comparable and both are (marginally) within the MINOS range of sensitivity, the OMSD model cannot be assumed and a generalised three-flavour analysis that involves six free parameters must be performed. The dependence of the oscillation probabilities on neutrino energy will be complex due to interference between the two Δm^2 's. The proposed low energy beam for MINOS will be required to measure Δm^2 .

CP VIOLATION: the CP violating amplitude that could be observed in MINOS if this scenario is assumed has been calculated in section 7.5 to be less than 10^{-3} and therefore unobservable.

Scenario 4: Three mass-scales, hierarchical mass spectrum

$$\Delta m_{43}^2 = 1 \text{ eV}^2, \Delta m_{32}^2 = 10^{-2} \text{ eV}^2, \Delta m_{21}^2 = 10^{-5} (10^{-10}) \text{ eV}^2$$

LSND: the LSND excess is explained by $\bar{\nu}_\mu \rightarrow \bar{\nu}_e$ oscillations with $\Delta m^2 \sim 1 \text{ eV}^2$ and $\sin^2 2\theta \sim 10^{-2}$.

ATMOSPHERIC: the atmospheric neutrino anomaly is explained by neutrino oscillations with $\Delta m^2 \sim 10^{-2} \text{ eV}^2$ and $\sin^2 2\theta \sim 1$. Oscillations in the mode $\nu_\mu \rightarrow \nu_\tau$ or $\nu_\mu \rightarrow \nu_s$ are possible, where ν_s is a sterile neutrino.

SOLAR: the solar neutrino problem can be solved by MSW or vacuum oscillations with $\Delta m^2 \sim 10^{-5}$ or $\Delta m^2 \sim 10^{-10} \text{ eV}^2$. An energy-dependent suppression of the neutrino flux is possible. It is possible to solve the solar neutrino problem with $\nu_e \rightarrow \nu_\tau$ or $\nu_e \rightarrow \nu_s$ oscillations.

MINOS ANALYSIS STRATEGY: this scenario assumes three independent mass scales so neither the OMSD model nor a generalised three-flavour framework can be assumed. A complex analysis involving four neutrino flavours (the three normal generations plus a sterile neutrino) which uses the oscillation probabilities observed by MINOS together with results from other experiments is therefore necessary.

CP VIOLATION: it has been shown [90] that the constraints on observing CP violation that are studied in section 7.5 are relaxed and a large CP violating effect could be observed in MINOS.

9.3 Implications of MINOS results

This thesis has demonstrated that it is possible to accurately measure the mixing parameters in MINOS if a large oscillation effect exists. It is interesting to consider what these results would imply for the underlying physics.

There are many theoretical models of neutrino mass and mixing that attempt to explain the current neutrino oscillation data in a consistent framework, for example [99][100][101][102] and the models described in [91]. This proliferation of models is due in part to the relative freedom in constructing physics beyond the Standard Model and also because the mixing parameters are not well-established by current experimental data. This second point is obviously an area in which MINOS could make a significant contribution. It is important to note that the models suppose that the current experimental hints of neutrino oscillations are in fact genuine effects. Many models assume the best-fit parameters from the Kamiokande atmospheric neutrino analysis ($\Delta m^2 \sim 0.01 \text{ eV}^2$ and $\sin^2 2\theta \sim 1$ [41]) are correct and, although the recent Super-Kamiokande result is suggestive of oscillations [36], it cannot

be said that the parameters (especially Δm^2) have been *measured* by either experiment. This thesis has shown that MINOS would be able to convincingly demonstrate the existence of neutrino oscillations with these parameters and measure the values of Δm^2 and $\sin^2 2\theta$.

Once oscillations have been established, the more detailed predictions of the models can be tested. This will be carried out by a number of experiments, including MINOS. The most recent models, for example [99], assume that the LSND effect, the atmospheric neutrino anomaly and the solar neutrino problem are all due to neutrino oscillations. This scenario is most easily explained by the mixing of four neutrino species (the three standard generations plus a sterile neutrino). A three-generation solution can be found although this requires that the atmospheric neutrino anomaly is due to large Δm^2 oscillations [56]. This result will be completely checked by MINOS, which can provide a direct measurement of Δm^2 up to 0.2 eV^2 and can also indicate whether Δm^2 is larger than this value.

The LSND result will be checked by the KARMEN experiment within the next few years and this will indicate whether three-generation or four-generation mixing models are appropriate. Several of the four-generation models make different predictions for the oscillation mode responsible for the atmospheric neutrino anomaly. This freedom is due to the poor discrimination between $\nu_\mu \rightarrow \nu_\tau$ and $\nu_\mu \rightarrow \nu_e$ oscillations offered by atmospheric neutrino experiments. The recent CHOOZ result [47] has already ruled out several mixing schemes that predict large $\nu_\mu \rightarrow \nu_e$ mixing for atmospheric neutrinos [57][102]. MINOS, which will have electron and tau identification abilities, will also be in a situation to discriminate between models that predict large $\nu_\mu \rightarrow \nu_\tau$ mixing [100][101] and those that

predict large $\nu_\mu \rightarrow \nu_s$ mixing, where ν_s is a sterile neutrino¹⁴ [99]. MINOS should also be able to probe $\nu_\mu \rightarrow \nu_e$ mixing below the CHOOZ limit and provide further constraints on possible oscillation models.

The spectrum of neutrino masses is not well-determined by current experiments. MINOS will be able to measure or constrain the value of one Δm^2 but, since a measurement of Δm^2 is only sensitive to the *differences* between neutrino mass eigenstates, this does not automatically distinguish between models with a strongly-ordered see-saw mass hierarchy or models with almost degenerate neutrino masses. It has recently been pointed out, however, [103] that neutrino oscillation experiments can provide strong constraints on the mass of possible Majorana neutrinos (even though oscillations do not distinguish between Dirac and Majorana neutrinos). The effective Majorana mass, $|\langle m \rangle|$, which is proportional to the matrix element for double-beta decay, is related to the matrix element U_{e3}^2 and the value of Δm^2 by the following expression, if the neutrino masses are strongly-ordered [103]:

$$|\langle m \rangle| \approx |U_{e3}|^2 \sqrt{\Delta m^2}. \quad (9.1)$$

An analysis of current neutrino oscillation data sets a limit of $|\langle m \rangle| < 3 \times 10^{-2}$ eV [103]. This limit depends on the value of Δm^2 and can therefore be further refined if a precision measurement of Δm^2 is made by MINOS together with a measurement or limit on the matrix element U_{e3}^2 from a search for $\nu_\mu \rightarrow \nu_e$ oscillations. Future double-beta decay experiments are only sensitive to $|\langle m \rangle| > 10^{-1}$ eV so if they observe a signal the pattern of neutrino masses is not hierarchical and the masses cannot be generated by the see-saw mechanism [103].

¹⁴ If $\nu_\mu \rightarrow \nu_s$ oscillations occur with $\Delta m^2 \sim 10^{-2}$ eV² and $\sin^2 2\theta \sim 1$ then MINOS is expected to observe a large, energy dependent, suppression of the ν_μ flux (as shown in the bottom-right plot of Figure 4.12) but no electron or tau appearance signals.

It is therefore clear that MINOS will be able to provide important information which will a) either establish or refute neutrino oscillations with parameters similar to those suggested by the Kamiokande atmospheric neutrino analysis; b) measure or set limits on the oscillation parameters which will test current models of neutrino mass and mixing and possibly indicate what lies beyond the Standard Model and c) indicate (when combined with the results of other experiments) what future experiments should be performed to further explore neutrino oscillation parameter space.

In conclusion, the future results of MINOS, in particular the ability to measure the mixing parameters, as described in this thesis, are of central relevance to the resolution of the atmospheric neutrino problem. The outcome of a search for neutrino oscillations in MINOS, whether positive or negative, will have far-reaching consequences for neutrino oscillation phenomenology.